



On the Absence of Stereoselectivity in the Catalytic Oxidation of Alkenes with a Surface-Bound Metalloporphyrin-Peptide Conjugate

G. Richard Geier III,^a Terry P. Lybrand,^b and Tomikazu Sasaki^{a*}

^aDepartment of Chemistry, University of Washington, Seattle, WA 98195-1700 (USA)

^bDepartment of Bioengineering and Department of Chemistry, University of Washington, Seattle, WA 98195 (USA)

Received 25 September 1998; revised 9 December 1998; accepted 15 December 1998

Abstract

As reported in the proceeding paper, the catalytic oxidation of alkene substrates using a novel surface-bound metalloporphyrin-peptide conjugate catalyst occurred largely in accord with the catalyst design. Yet despite the regulation of many aspects of the oxidation, the asymmetric conjugate catalyst did not oxidize substrates stereoselectively. The absence of stereoselective catalysis is considered here through examination of potential experimental problems (improper surface assembly and catalyst degradation) and potential design problems (binding pocket symmetry and peptide packing). Neither experimental issue was shown to be the definitive problem. Molecular modeling of the catalyst suggested the binding pocket was too symmetrical. © 1999 Elsevier Science Ltd. All rights reserved.

Keywords: stereoselectivity; molecular modeling; catalysis; porphyrins

Introduction

In the first paper in this series [1], we reported the results of oxidation experiments using a surface-bound Mn(III)porphyrin-peptide conjugate catalyst (Figure 1). The conjugate catalyst was able to mediate the oxidation of alkene substrates in good yield under a variety of conditions. In addition, the oxidation reactions showed expected substrate discrimination based on substrate size, as well as perturbation of oxidation product ratios. The magnitude of substrate size discrimination and product ratio perturbation was solvent influenced. All results indicated that catalysis occurred between the porphyrin ring and the peptide chain, with the peptide influencing the outcome of the reaction in accord with the catalyst design. This paper

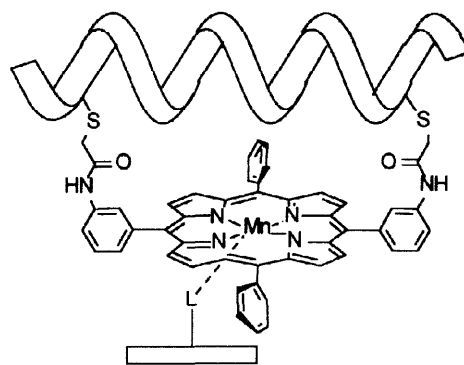


Figure 1. Surface bound Mn(III)porphyrin-peptide conjugate.

* To whom correspondence should be addressed. E-mail: sasaki@macmail.chem.washington.edu. Fax: (206) 685-8665.

considers the stereochemical outcome of those oxidations. Given the apparent interaction of the substrate with the peptide portion of the catalyst and the asymmetric nature of the α -helical peptide, we expected at least some stereoselectivity. Interestingly, none was observed. Explanations for the surprising absence of stereoselective catalysis are discussed.

Results and Discussion

Stereochemistry of Mn(III)porphyrin-Peptide Conjugate Mediated Oxidation Reactions

After the initial analysis of the oxidation products by $^1\text{H-NMR}$, the chiral NMR shift reagent $\text{Eu}(\text{hfc})_3$ was added to the NMR sample. The shift reagent resolved the enantiomeric proton resonances and the relative amounts of each enantiomer was determined by peak integration. All of the oxidation experiments involving prochiral substrates reported in the previous paper [1] resulted in no significant enantiomeric excess. The detection limit for enantiomeric excess under the conditions of this study was 5-10% ee. This result was surprising as other observations (lowered yields, perturbed product ratios, and substrate discrimination) were supportive of the catalyst design. Given the chirality of the amino acid residues and the asymmetry of the peptide conformation, the absence of stereoselectivity was unexpected.

Experimental Explanations for Non-Enantioselectivity

In order to understand the catalyst's deficiency, potential experimental explanations were examined. Improper surface assembly was one possible explanation. The differences in the oxidation results between the Mn(III)conjugate and the Mn(III)TPP reported in the previous paper argue against glaring problems with the deposition of the Mn(III)conjugate on the modified silica gel (if the surface had associated with the peptide rather than with the unhindered face of the porphyrin ring, oxidation would have occurred from the unhindered face producing oxidation results in line with the results from the unhindered Mn(III)TPP). Nevertheless, the precise structure of the Mn(III)conjugate on the support was unknown so we could not be certain interaction with the surface did not perturb the structure of the Mn(III)conjugate in an undesired fashion. To address this issue, solution oxidation experiments were performed using dissolved rather than surface-bound catalyst. The scale and reactant ratios were the same as in the surface-bound experiments, styrene was used as the substrate, and 50% aqueous isopropanol solvent system was used for catalyst solubility. Experiments were performed in the presence and absence of a bulky nitrogenous ligand, 1,5-dicyclohexylimidazole. Although differences in yield and product ratios comparable to the surface-bound experiments were observed between the Mn(III)conjugate and Mn(III)TPP, once again no stereoselectivity was observed [2]¹. The solution experiments suggest the behavior of the surface-bound catalyst was as desired, with oxidation occurring from the hindered face.

Catalyst degradation leading to loss of stereoselectivity was a second potential experimental problem. Oxidative modification and degradation of the catalyst is a well known problem with artificial metalloporphyrin catalysts [3], thus, it was very reasonable to expect some catalyst degradation to have occurred. As degradation proceeds, the stereodiscriminating ability of the peptide may decrease [4]. Catalyst degradation was monitored in our experiments in three ways: UV-vis, HPLC, and amino acid analysis. UV-vis analysis of post-oxidation Mn(III)conjugate showed loss of porphyrin absorbance. Typical values were about 40% loss in

¹ Additional interesting observations not central to this paper were made and are described elsewhere in detail [2].

chloroform experiments, 50% loss in aqueous isopropanol, and 60% loss in buffer. The precise values depended on the reactivity of the substrate. Clearly, degradation of the porphyrin occurred. RP-HPLC analysis of post-oxidation Mn(III)conjugate allowed determination of the diversity of degraded catalyst species. The appearance of the chromatogram depended on substrate reactivity. The more reactive substrates led to less degradation of the catalyst and to cleaner HPLC chromatograms. Yet, even the best chromatogram showed significant degradation. The degradation products formed a plethora of new peaks, so no attempt was made to specifically identify the new materials. The RP-HPLC runs were monitored at 477 nm, the Soret band of the porphyrin ring. Thus, only species with intact porphyrin rings were detected. This indicates modification in addition to porphyrin ring degradation occurred to the catalyst. Amino acid analysis provided more specific information regarding the modification of the individual amino acid residues. In the chloroform experiments, no consistent pattern of degradation was observed as no amino acid ratio was consistently lower than the others. In nearly all of the experiments in both aqueous solvents, the ratio of leucine residues was one to two lower than the expected theoretical ratio of four. Thus, in those solvents the leucine residues appeared to suffer more oxidative modification than the other residues. Although modification of the catalyst was not desired, the way in which the modification occurred was consistent with the design of the catalyst. The leucine residues should be positioned closest to the metal center of the porphyrin ring [5], thereby being the most prone to oxidation [6,7].

The effect the degradation had on the stereochemical outcome of the oxidation reaction was uncertain. First, it was important to know if the catalytic activity decreased as modification occurred. If the catalyst ceased to function after very limited modification, the effect of the degradation on the enantioselectivity would be less than if the catalyst continued to oxidize substrate after having been compromised. An experiment was performed where the Mn(III)conjugate catalyst was subjected to two rounds of oxidations in 50% aqueous isopropanol with styrene as the substrate. The scale of the reactions and ratios of reactants were identical to previous experiments. After the first oxidation experiment, the catalyst was recovered and used a second time. The yield of oxidized styrene decreased very little from the first experiment to the second, 60% and 50% respectively.

Given those results, it was important to obtain oxidation results under conditions where little degradation occurred. One approach is to decrease the possible turnover number of the catalyst. In fact, Mansuy, et. al. have performed some reactions under an average turnover number of five [8]. Unfortunately, limited Mn(III)conjugate ruled out extensive low turnover oxidation experiments. An experiment was performed at a catalyst to substrate to PhIO ratio of 1 : 300 : 30, in 50% aqueous isopropanol using 90 nmol of catalyst. The typical lower oxidation yield for the Mn(III)conjugate versus Mn(III)TPP reaction was observed, and the magnitude of the difference was the same as in previous experiments at higher turnover. Once again, no enantiomeric excess was detected. The post-oxidation analysis of the Mn(III)conjugate/IPS showed very little degradation occurred under the lower turnover conditions. The RP-HPLC chromatogram was very clean and amino acid analysis provided the theoretical ratios. In this experiment, the absence of stereoselectivity could not be tied directly to catalyst degradation.

Additional secondary experimental concerns were also considered. (1) The peptide packing with the porphyrin ring was potentially variable. Although CD spectroscopy suggested high helical secondary structure content, the packing between the peptide and the porphyrin ring may be variable. Studies with three helix bundle systems have shown high secondary structure content does not necessarily mean a stable tertiary structure has been obtained [9]. Variable packing could produce a variety of substrate binding pockets leading to absence of stereoselectivity. Although much of the data collected were consistent with the peptide being

reasonably structured in the desired orientation, the data did not entirely rule out this concern. (2) The substrate pool was limited. Although a number of substrates were examined, the list was far from exhaustive.² It is possible substrates exist that may be oxidized stereoselectively by the catalyst as other reports show the degree of enantioselectivity for a particular catalyst varies with the substrate [10]. Yet, typically variances of 70% ee to 0% ee are not observed, so we hesitate to place all of the blame on substrate selection.

Design Explanations for Non-Enantioselectivity

Although some potential experimental problems (catalyst degradation) exist, those concerns were not the definitive source of the non-enantioselectivity. In fact, much of the evidence suggested the catalyst performed about as well as its design allowed. Thus, the design of the porphyrin-peptide conjugate catalyst was re-examined with the aid of computer molecular modeling. The potential design problems fell into three major areas—poor substrate binding pocket dimensions, a too symmetrical binding site, and poor peptide-porphyrin packing.

The porphyrin-peptide conjugate model was constructed using standard templates found in *Insight[®] II* with the peptide assembled in an ideal α -helical conformation. The qualitative features of the binding site were examined. In agreement with the modeling done at the onset of the project, the binding site appeared to be reasonable (Figure 2). The leucine side chains determined the physical dimensions of the binding site, with two of the four groups lying slightly closer to the center of the porphyrin. The other side chains all projected away from the porphyrin ring. The axis of the helix lay an appropriate distance above the porphyrin ring

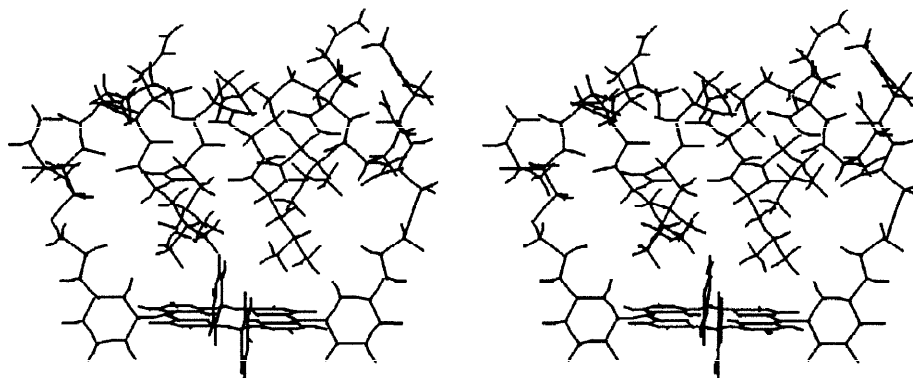


Figure 2. Stereoview of the porphyrin-peptide conjugate showing four leucine side chains defining the binding site.

The symmetry of the binding site was considered as attempts were made to dock substrates into the binding site. During the docking trials, substrates could be introduced in a variety of orientations. In order to learn how to best place substrates into the binding site, docking studies were performed for a variety of catalyst structures reported in the literature to perform successful asymmetric epoxidation [4,8,10c-e,11]. As it is known which enantiomer is formed in greater excess, the docked structures could be checked. Unfortunately, attempts to predict the stereochemical outcome for each catalyst were not very successful. Nevertheless, the catalyst structures were compared for similarities and differences by superimposing each literature structure onto the porphyrin-peptide conjugate. Figure 3 shows overlays of the

² The substrate pool selected for this study was limited by three concerns. The substrates had to be suitably reactive to produce enough oxide to quantify by ¹H NMR at a low catalyst scale. The substrates had to be somewhat soluble in the most promising aqueous solvents. The substrates could not bear functional groups that would interfere with NMR analysis and the chiral shift reagent.

conjugate with three successful asymmetric catalysts [4,10e]. The positioning of the auxiliary groups between the structures was strikingly similar. The leucine residues of the peptide lined up very well with the auxiliary groups of the literature systems. In fact, comparison with a recent catalyst reported by Collman's group [4] (Figure 3a) allows one to trace the strap of Collman's catalyst up a leucine residue, along the peptide backbone, and back down a second leucine side chain. Based on this analysis, the successful asymmetric catalysts had spacing and positioning of the auxiliary groups very similar to our own. So how was our catalyst different?

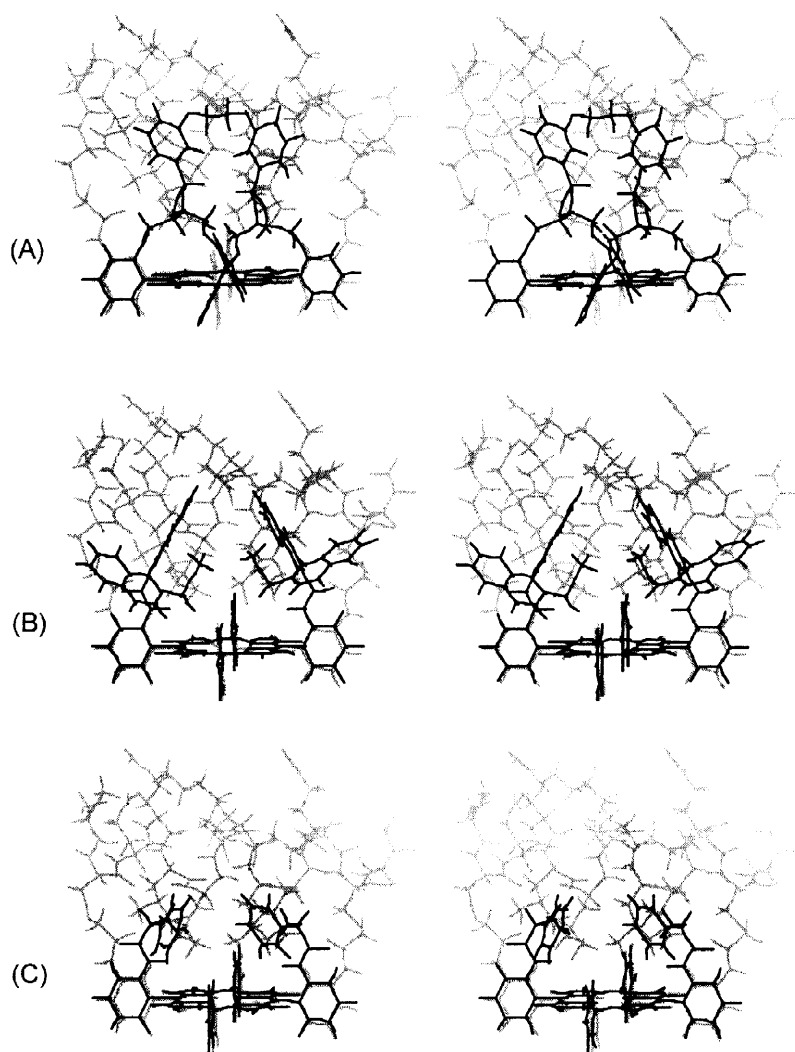


Figure 3. Stereoviews of the conjugate (gray) superimposed with successful asymmetric catalysts (black). (A) Reference 4. (B) Reference 10e. (C) Reference 10e.

If one were to divide the porphyrin plane into quadrants, the model systems all had appendages blocking two of the quadrants while the other two were left open (Figure 4a). In addition, the two blocked quadrants are located diagonally from one another. Regardless of the approach of the substrate, the opening is encountered in the same fashion. Unlike the other catalysts, the conjugate placed bulky leucine groups in such a way as to block all four quadrants (Figure 4b). As the result, the substrate may have no clearly preferred route of entry,

leading to a racemic product. Support for this conclusion has recently been provided in a report detailing oxidation studies using picket fence porphyrins of variable substitution [12].

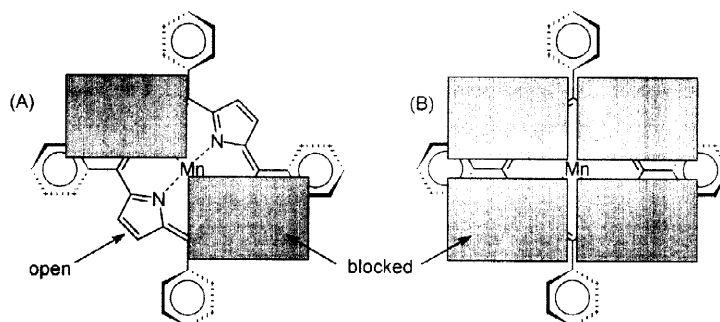


Figure 4. Illustration of the blocking of substrate approach in (A) successful asymmetric catalysts and in (B) the conjugate.

An examination of the binding site symmetry also led to a more subtle observation. When considering the likely route of entry for the substrate, initial intercalation of the substrate's aromatic ring between the two leucine residues is reasonable [10a,c,e,13]. Substrate binding in the model structure (Figure 5a) would have to tilt the same way regardless of the particular side of approach. The alkene would be presented to the oxo group in a consistent fashion. The conjugate (Figure 5b) requires the substrate to tilt in opposite directions due to the propagation of the helix backbone, projecting the side chains in such a way that the front and back sides are different. Thus, the alkene would be presented to the oxo group in a pseudo-mirror image fashion leading to racemic oxidation.

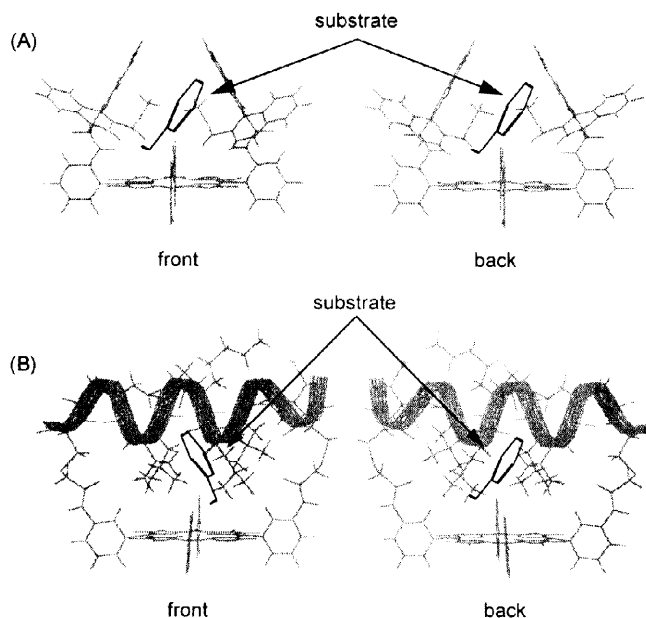


Figure 5. Comparison of substrate (styrene) binding from the front and back sides. (A) A successful asymmetric catalyst [10e]. (B) The conjugate.

Since there is some limited conformational flexibility for the porphyrin-peptide conjugate, molecular dynamics simulations were performed for the conjugate and conjugate-substrate

complexes. The general mobility of the leucine side chains, the position of the peptide across the helix, and the mobility of docked substrates were examined. Very early in the simulation, the peptide chain flopped over to one side (Figure 6), and stayed tipped during the remainder of the trajectory. Although that behavior is most likely exaggerated in the gas phase calculations³, nevertheless, some listing of the peptide across the porphyrin face is reasonable given the chirality of the helix and of the linking cysteine residues. In fact, during the model building, the peptide consistently listed toward the right when viewed down the helix axis with the C-terminus placed closest to the viewer. There are at least two important consequences of such asymmetry: (1) substrate approach from one direction should be favored over approach from the other, (2) the precise dimensions of the substrate binding pocket may be variable. Clearly, the second point could negatively impact stereoselectivity.

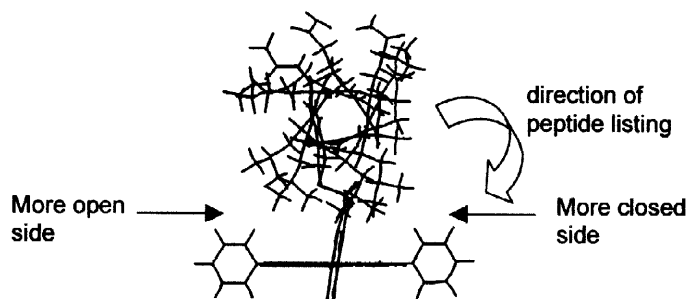


Figure 6. View of the conjugate showing the direction of peptide listing.

Additional dynamics simulations were performed with the conjugate containing docked substrates (styrene, *cis* stilbene, or 2,4,6-trimethylstyrene). When substrate was placed in the more open side, the intercalated substrate rapidly pushed one of the leucine side chains out of the way so the substrate could adopt a parallel orientation relative to the porphyrin ring, with the aromatic ring of the substrate residing above one of the pyrrole rings of the porphyrin. This orientation placed the alkene directly over the center of the porphyrin ring and would require a top-on transition state structure. This result suggests that designing specific pockets to bind the aromatic ring might increase the enantioselectivity. In order to accommodate the substrate, the helix backbone moved slightly away from the porphyrin placing substrate in a hydrophobic pocket defined by the leucine residues. Those major changes occurred during the first 5 ps of the dynamics simulations. The substrate orientation remained constant during the remainder of the simulations. Docking the substrate in the more closed side of the conjugate led to a very different result. From that starting point, the substrate was immediately pushed across the porphyrin ring toward the more open side. Then it settled into an orientation similar to that observed in the previous simulations. In these simulations, the peptide clearly forced the substrates to move toward the more open side. The simulations suggest binding to the two sides of the conjugate is not equivalent. Thus, designing a specific pocket to bind the substrate's aromatic ring on the more open side of the binding pocket may have a greater impact on enantioselectivity.

Conclusions

The absence of stereoselectivity observed in the catalytic oxidation of alkenes using the Mn(III)porphyrin-peptide conjugate led to consideration of possible experimental and design explanations. Although the structure of the surface-bound Mn(III)conjugate was uncertain and degradation of the catalyst clearly occurred, neither experimental issue could be shown to be the definitive problem. A re-examination of the design of the conjugate catalyst pointed to

³ In water, there is likely a greater driving force for maintaining a hydrophobic core, requiring the peptide to remain more centered.

some potential issues. Especially helpful was a comparison made to successful asymmetric catalysts reported in the literature. Based on the molecular modeling studies, questions were raised regarding the symmetry of the substrate binding pocket and the packing of the peptide chain across the porphyrin ring. Those observations may now be examined simply by altering the amino acid sequence of the peptide chain. This synthetic flexibility highlights a major potential strength of the porphyrin-peptide approach. If a stereoselective catalyst can be generated simply by altering the amino acid sequence so as to create an asymmetric binding pocket, it would suggest the chirality of the amino acid residues and of the peptide helix in this initial catalyst were insufficient to produce asymmetric catalysis. In addition to such asymmetry, the precise positioning and packing of the side chains may be crucial [14].

Experimental

General Methods

Refer to the previous paper for general experimental details [1].

Determination of Enantiomeric Excess

After performing the reaction, work-up, and initial analysis as described in the previous paper, enantiomeric excess was determined by integration of the ^1H NMR spectrum obtained after addition of $\text{Eu}(\text{hfc})_3$ (Aldrich). The shift reagent was added in 1-10 mg aliquots until the enantiomeric resonances were resolved. Reactions performed in CDCl_3 required about 3-5 mg of shift reagent, reactions in 50% *i*-PrOH required 30-40 mg, and reactions performed in buffer required 10-15 mg.

Mn(III)Conjugate Solution Oxidation Experiment

A stock solution of Mn(III)conjugate was prepared in 50% aqueous MeOH. The concentration of the solution was determined spectroscopically ($\epsilon_{466} = 1.03 \times 10^5 \text{ M}^{-1}\text{cm}^{-1}$). To a pair of 5-ml pear shaped flasks, 15 nmol of Mn(III)conjugate was added. The samples were lyophilized to dryness. A similar procedure was followed to prepare two flasks containing 15 nmol of Mn(III)TPP. To all four flasks, 60 μL of 50% *i*PrOH- d_8 in pH 7 phosphate buffer and 3.4 μL (30 μmol) styrene were added. To one of each pair of Mn(III)conjugate and Mn(III)TPP flasks, 0.87 mg (3.75 μmol) dicyclohexylimidazole (Aldrich) was added. All reactions were stirred for a few minutes under argon at room temperature, then 0.66 mg (3.0 μmol) ground PhIO was added. The reaction, work-up and analysis were done as described in the first paper.

Mn(III)Conjugate Catalyst Recovery Experiment

A Mn(III)conjugate/IPS oxidation experiment was performed as previously described with styrene as the substrate. After the reaction was complete, the silica was rinsed three times with CDCl_3 . The once used Mn(III)conjugate/IPS was transferred back into a 5-ml pear shaped flask, and the oxidation procedure was performed a second time.

Mn(III)Conjugate/IPS Low Catalyst Turnover Oxidation Experiment

To a 5-ml pear shaped flask, 18 mg (90 nmol) of Mn(III)conjugate/IPS was transferred. To that flask, 120 μL of 50% iPrOH solvent and 3.0 μL (26 μmol) of styrene were added. The solution was stirred under argon for a few minutes, then 0.57 mg (2.6 μmol) ground PhIO was added. The reaction, work-up, and analysis were performed as previously described.

Post-Oxidation Evaluation of Mn(III)Conjugate/IPS

Evaluation of Mn(III)conjugate/IPS after oxidation experiments was performed three ways. (1) UV-vis analysis: after the oxidation was complete the Mn(III)conjugate/IPS was treated with glacial acetic acid to remove the Mn(III)conjugate from the silica. The solution was filtered, rinsed thoroughly, and diluted in a 5-ml volumetric flask. The absorbance at 472 nm was found for the resulting solution and comparison was made to the theoretical value. (2) RP-HPLC analysis: post-oxidation Mn(III)conjugate/IPS was rinsed three times with water, three times with acetone, followed by three rinses with methylene chloride. The sample was allowed to air dry while shielded from the light. The Mn(III)conjugate was released from a small sample of the IPS using 5 drops of acetic acid. About 20 μL of the solution was injected onto a C4 analytical column (Microsorb-MV, Rainin). A linear gradient of 40% B to 60 % B over 15 minutes was used. The detector was set at 470 nm. Mn(III)conjugate eluted at about 15 minutes. Most degradation products eluted earlier in a broad hump. (3) Amino acid analysis: a small amount of the rinsed post-oxidation Mn(III)conjugate/IPS was placed into amino acid analysis tubes. Control samples of Mn(III)conjugate/IPS were also included. The analysis was performed as previously described [1].

Molecular Modeling

Models of the porphyrin-peptide conjugate were constructed with *Insight*[®] II [15], using standard *Insight* molecular fragment templates. All energy minimization and molecular dynamics calculations were done in the gas phase with a distant dependent dielectric constant and the CFF potential energy functions. Minimization was performed using the steepest descents algorithm followed by the conjugate gradient minimization algorithm. Minimization was continued until the RMS derivative was less than 0.10 kcal/mol/Å.

The peptide fragment was constructed as an ideal α -helix, and minimized prior to attachment to the porphyrin ring. The glutamic acid and lysine side chains were constrained initially to form two salt bridges in the helix. The pH of the system was set to neutral, and only the helix side chains were allowed to move in the initial energy minimization. Then, the peptide was attached to the porphyrin ring and the completed porphyrin-peptide conjugate structure was energy minimized. This structure served as the template for other experiments. Models for the successful asymmetric catalysts reported in the literature were constructed in a similar fashion. For bis-faced systems, only a single face was constructed.

The substrate binding sites for all of the models were examined by generating solvent accessible surfaces. A variety of substrates were docked manually, using the “bump” operation in *Insight*[®] II which finds unfavorable van der Waals contacts. Different structures were compared graphically after structural superposition.

Dynamics trajectories were calculated for the free base conjugate, and for conjugate with bound styrene, cis stilbene, and 2,4,6-trimethylstyrene. Prior to dynamics, the conjugate with the bound substrate was energy minimized with no constraints. Dynamics simulations were

performed for 100 ps, using a leapfrog integration algorithm with a 1 fs time step. The trajectories were analyzed visually using *Insight*[®] II.

Acknowledgment

GRG was supported by a NIH training grant (5T326M0437) and by scholarships from the NCAA and the ARCS foundation. All molecular modeling work was performed in the Whitaker Molecular Modeling Laboratory in the Department of Bioengineering.

References

1. Geier, G. R.; and Sasaki, T. *Tetrahedron* **1999**, *55*, 1859.
2. Geier, G. R. *The Preparation of a Metalloporphyrin-Peptide Conjugate Artificial Protein for the Catalytic Oxidation of Alkenes*. University of Washington, 1997.
3. (a) Sheldon, R. A., Ed., *Metalloporphyrins in Catalytic Oxidations*; Marcel Dekker, Inc.: New York, **1994**. (b) Montanari, F., and Casella, L., Eds., *Metalloporphyrins Catalyzed Oxidations*; Kluwer Academic Publishers: Boston, **1994**. (c) Collman, J. P.; Zhang, X.; Lee, V. J.; Uffelman, E. S.; and Brauman, J. I. *Science* **1993**, *261*, 1410. (d) Montanari, F.; Banfi, S.; Pozzi, G.; and Quici, S. *Rev. Heteroatom Chem.* **1992**, *6*, 94. (e) Meunier, B. *Chem. Rev.* **1992**, *92*, 1411. (f) Gunter, M. J.; and Turner, P. *Coord. Chem. Rev.* **1991**, *108*, 115. (g) White, P. W. *Bioorg. Chem.* **1991**, *18*, 440.
4. Collman, J. P.; Lee, V. J.; Kellen-Yuen, C. J.; Zhang, X.; Ibers, J. A.; and Brauman, J. I. *J. Am. Chem. Soc.* **1995**, *117*, 692.
5. Geier, G. R.; and Sasaki, T. *Tetrahedron Lett.* **1997**, *38*, 3821.
6. Groves, J. T.; Nemo, T. E.; and Myers, R. S. *J. Am. Chem. Soc.* **1979**, *101*, 1032.
7. (a) Groves, J. T.; Kruper, W. J.; Nemo, T. E.; and Myers, R. S. *J. Mol. Catal.* **1980**, *7*, 169. (b) Chang, C. K.; and Kuo, M. S.; *J. Am. Chem. Soc.* **1979**, *101*, 3413.
8. Mansuy, D.; Battioni, P.; Renaud, J. P.; and Guerin, P. *J. Chem. Soc. Chem. Commun.* **1985**, 155.
9. Lieberman, M.; Tabet, M.; and Sasaki, T. *J. Am. Chem. Soc.* **1994**, *116*, 5035.
10. (a) Naruta, Y.; Ishihara, N.; Tani, F.; and Maruyama, K. *Bull. Chem. Soc. Jpn.* **1993**, *66*, 158. (b) Collman, J. P.; Zhang, X.; Lee, V. J.; and Brauman, J. I. *J. Chem. Soc. Chem. Commun.* **1992**, 1647. (c) Groves, J. T.; and Viski, P. *J. Org. Chem.* **1990**, *55*, 3628. (d) Naruta, Y.; Tani, F.; and Maruyama, K. *Chem. Lett.* **1989**, 1269. (e) Groves, J. T.; and Myers, R. S. *J. Am. Chem. Soc.* **1983**, *105*, 5791.
11. (a) Collman, J. P.; Lee, V. J.; Zhang, X.; Ibers, J. A.; and Brauman, J. I. *J. Am. Chem. Soc.* **1993**, *115*, 3834. (b) Collman, J. P.; Zhang, X.; Lee, V. J.; and Brauman, J. I. *J. Chem. Soc. Chem. Commun.* **1992**, 1647.
12. Rose, E.; Soleilhavoup, M.; Christ-Tommasino, L.; Moreau, G.; Collman, J.P.; Quelquejeu, M.; and Straumanis, A. *J. Org. Chem.* **1998**, *63*, 2042.
13. (a) Groves, J. T.; and Nemo, T. E. *J. Am. Chem. Soc.* **1983**, *105*, 5786. (b) Naruta, Y.; Ishihara, N.; Tani, F.; and Maruyama, K. *J. Am. Chem. Soc.* **1991**, *113*, 6865. (c) Ostovic, D.; He, G. X.; and Bruce, T. C. In *Metalloporphyrins in Catalytic Oxidations*; Sheldon, R. A., Ed.; Marcel Dekker, Inc.: New York, **1994**, 29–68. (d) Ostovic, D.; and Bruce, T. C. *Accs. Chem. Res.* **1992**, *25*, 314.
14. Sanders, J. K. M. *Chem. Eur. J.* **1998**, *4*, 1378.
15. Computational results obtained using software programs from Biosym/MSI of San Diego—dynamics calculations were done with the *Discover*[®] program, using the CFF91 forcefield, and graphical displays were printed out from the *Insight*[®] II molecular modeling system.